Telomere dynamics in Fancg-deficient mouse and human cells

Sonia Franco, Henri J. van de Vrugt, Piedad Fernández, Miguel Aracil, Fre Arwert, and María A. Blasco

A number of DNA repair proteins also play roles in telomere metabolism. To investigate whether the accelerated telomere shortening reported in Fanconi anemia (FA) hematopoietic cells relates to a direct role of the FA pathway in telomere maintenance, we have analyzed telomere dynamics in *Fancg*-deficient mouse and human cells. We show here that both hematopoietic (stem and differentiated bone marrow cells, B and T lymphocytes) and nonhematopoietic (germ cells, mouse embryonic fibroblasts [MEFs]) *Fancg*$^{-/-}$ mouse cells display normal telomere length, normal telomerase activity, and normal chromosome end-capping, even in the presence of extensive clastogen-induced cytogenetic instability (mitomycin C [MMC], gamma-radiation). In addition, telomerase-deficient MEFs with humanlike telomere length and decreased Fancg expression (G5 *Terc*$^{-/-}$*/Fancg* shRNA3 MEFs) display normal telomere maintenance. Finally, early-passage primary fibroblasts from patients with FA of complementation group G as well as primary human cells with reduced FANCG expression (*FANCG* shRNA IMR90 cells) show no signs of telomere dysfunction. Our observations indicate that accelerated telomere shortening in patients with FA is not due to a role of FANCG at telomeres but instead may be secondary to the disease. These findings suggest that telomerase-based therapies could be useful prophylactic agents in FA aplastic anemia by preserving their telomere reserve in the context of the disease. (Blood. 2004;104:3927-3935)

Introduction

Telomeres are specialized heterochromatic regions that cap linear chromosomes, buffering the loss of telomeric DNA with cell replication.[1] In addition, telomeres guarantee genomic stability by preventing recognition of chromosome termini as broken DNA ends.[1] It has been proposed that telomere capping relies on the ability of specialized telomeric proteins, such as Pot1 and TRF2, to stabilize a T-loop structure formed by folding back of the most distal single-stranded telomeric 3′-overhang into double-stranded telomeric DNA.[2] In addition, proteins known for their roles in several specialized DNA repair pathways, such as nonhomologous end-joining (NHEJ) or homologous recombination (HR), have recently been shown to actively participate in telomere maintenance in normal cells, by either stabilizing telomere structure and/or regulating the access of telomerase to the 3′-overhang.[3-11]

Telomerase is a reverse transcriptase that elongates telomeres using a built-in RNA as a template.[12] Telomerase activity is detected in hematopoietic stem cells and lymphocytes.[13] In the absence of telomerase, telomere attrition ensues rapidly and results in bone marrow failure in both human beings[14,15] and mice.[16,17] Significantly, accelerated telomere shortening is also common in forms of aplastic anemia with no known defects in telomere maintenance,[18,19] and it is thought to result from increased cell turnover and perhaps damage to telomeric DNA by abnormal metabolic by-products.[20] Fanconi anemia (FA) is a congenital syndrome that features aplastic anemia and progression to leukemia early in life, hypogonadism, developmental abnormalities, and epithelial cancers.[21] The syndrome is genetically heterogeneous, with 11 complementation groups and 8 genes cloned to date; however, a defect in DNA interstrand cross-link (ICL) repair is common to all groups.[22] Moreover, the function of FA proteins is closely linked to that of proteins involved in DNA damage signaling, such as ATM and ATR, and homology-directed DNA repair, such as RAD51, BRCA1 and BRCA2,[23] some of which participate in telomere maintenance as well. These observations, together with prior reports showing that telomere shortening is accelerated in hematopoietic cells and fibroblasts of patients with Fanconi anemia,[24-28] led us to investigate whether the FA pathway is involved in telomere maintenance.

FANCG/XRCC9 is a 65-kDa protein with at least 7 protein-protein interaction tetratricopeptide repeat (TPR) motifs.[29,30] Together with Fanconi proteins A, C, E, F, and L, FANCG forms a nuclear core complex that monoubiquitinates FANCD2, which is then recruited to DNA repair foci and S-phase foci, where it colocalizes with BRCA1 and Rad51.[23] In addition, FANCG has been shown to interact directly with BRCA2.[31] Mice deficient in *FANCG* previously generated by us show the FA-characteristic cross-linker sensitivity.[32] Moreover, mouse *fancg* is functional in human cells and mediates mitomycin C (MMC) resistance of FA-G

From the Molecular Oncology Program, Spanish National Cancer Centre (CNIO), Madrid, Spain; Department of Clinical Genetics and Human Genetics, VU University Medical Center, Amsterdam, The Netherlands; and Department of Immunology and Oncology (DIO), National Center of Biotechnology (CNB-CSIC), Campus de Cantoblanco, Madrid, Spain.

Submitted November 14, 2003; accepted August 5, 2004. Prepublished online as *Blood* First Edition Paper, August 19, 2004; DOI 10.1182/blood-2003-10-3626.

Supported by the Spanish Ministry of Science (SAF2001-1869, GEN2001-4856-C13-08), the Regional Government of Madrid (08.1/0054/01), European Union (TELOSENS FIGH-CT-2002-00217, INTACT LSHC-CT-2003-506803, ZINCAGE FOOD-CT-2003-506850, RISC-RAD FI6R-CT-2003-508842), and the Josef Steiner Award 2003. S.F. is a predoctoral fellow of the Fondo de Investigaciones Sanitarias (FIS). Also supported by the Dutch Cancer Society project VU-2000-2157 (H.J.V.).

The online version of the article contains a data supplement.

Reprints: María A. Blasco, Molecular Oncology Program, Spanish National Cancer Centre, 3 Melchor Fernández Almagro, 28029 Madrid, Spain; e-mail mblasco@cnio.es.

The publication costs of this article were defrayed in part by page charge payment. Therefore, and solely to indicate this fact, this article is hereby marked "advertisement" in accordance with 18 U.S.C. section 1734.

patient cell lines.[33] In addition, *Fancg*-deficient mice faithfully represent the compromised fertility that has also been reported to occur in human patients with FA.[32] However, like other disease mouse models, *Fancg*-deficient mice do not develop aplastic anemia, perhaps related to the fact that mouse telomeres are very long compared with those of human beings. A mouse with humanlike telomere length has been previously generated by us (*Terc*$^{-/-}$ mice[34]). In the absence of telomerase activity, late-generation (G5) *Terc*$^{-/-}$ cells display chromosomal ends without detectable telomere signals, which, like short telomeres in human cells, trigger cellular DNA damagelike responses.[35] We show here that *Fancg*$^{-/-}$ cells with long telomeres, as well as *G5 Terc*$^{-/-}$ cells with short telomeres in which Fancg expression is markedly decreased by RNA interference, display normal telomere maintenance in a wide range of tissues. Similar observations are drawn from the analysis of primary fibroblasts from patients with FA of the complementation group G and of human primary embryonic fibroblasts with reduced FANCG expression, leading us to conclude that mammalian telomere maintenance is not dependent on FANCG activities.

Materials and methods

Mice and cells

Fancg$^{-/-}$ mice were generated in a 129Ola/FVB background.[32] Different tissues were obtained from 2- to 4-month-old male mice (3 *Fancg*$^{+/+}$, 6 *Fancg*$^{+/-}$, and 6 *Fancg*$^{-/-}$ mice). Either *Fancg*$^{+/+}$ or *Fancg*$^{+/-}$ cells were used indistinctly as controls. Mouse embryonic fibroblasts (MEFs) (4 *Fancg*$^{+/+}$ and 4 *Fancg*$^{-/-}$ independent cultures) were obtained at E13.5 following standard procedures; all experiments were done at passage 2. G5 *Terc*$^{-/-}$ MEFs were from an Sv129/Bl6 background.[34] Primary fibroblasts from patients with FA of the complementation group G were EUFA 0636 (16-year-old male) and European Fanconi Anemia Center (EUFA) 1093-F (4-year-old male). IMR90 cells expressing the ecotropic receptor were a kind gift from Manuel Serrano, CNIO, Spain.

Isolation of stem cell–enriched bone marrow cells

Bone marrow (BM) cells from 3 age-matched *Fancg*$^{+/+}$ and 3 *Fancg*$^{-/-}$ females were flushed from femurs and tibiae, and low-density mononuclear cells (LDMNCs) were purified by centrifugation in a 3-density gradient (1.090, 1.080, and 1.050 g/mL) and prepared by mixing NycoPrep 1.077A (1.077 g/mL) and OptiPrep (1.320 g/mL) (Axis-Shield PoC, Oslo, Norway). LDMNCs were then incubated with purified rat antimouse monoclonal antibodies anti-CD4, anti-CD8, anti-B220, anti–Gr-1, anti–Mac-1, and anti–TER-119, all from BD PharMingen (San Diego, CA), followed by incubation with Dynabeads M-450 sheep antirat immunoglobulin G (IgG) (Dynal Biotech, Oslo, Norway). Lin$^+$ cells attached to beads were separated with a magnet; the remaining medium, containing the Lin$^-$ fraction, was collected and cells either flash frozen or fixed for telomere analysis.

Telomere length measurement

Flow–fluorescence in situ hybridization (flow-FISH). Fresh bone marrow cells (BMCs) and splenocytes were hybridized with a fluorescein isothiocyanate (FITC)–labeled telomeric peptide nucleic acid (PNA) probe.[36] Telomere fluorescence of at least 5000 G_0/G_1-gated cells was measured using a Coulter flow EPICS XL cytometer (Beckman Coulter, Marseille, France). For conversion of arbitrary units of fluorescence to kilobase pairs (kbp), the murine lymphoma cell lines L5178Y and L5178Y-S, of known telomere lengths, were assayed in parallel to generate a telomere length regression line.[37]

Telomere restriction fragments (TRFs). BMCs, splenocytes, and MEFs were directly embedded into agarose plugs. For tissue analysis, nuclei were obtained as described.[38] Pulse field electrophoresis and hybridization with a telomeric probe were done as described.[34]

Quantitative telomeric fluorescence in situ hybridization (Q-FISH). Standard methanol/acetic acid–fixed metaphase preparations were hybridized with a cyanine 3 (Cy3)–labeled PNA telomeric probe in 70% formamide and counterstained with DAPI (4,6 diamidino-2-phenylindole) as previously described.[39] Images were captured using a COHU CCD camera on a fluorescence microscope (Leitz DMRB; Leica, Heidelberg, Germany). For telomere length measurement, integrated telomere fluorescence signal of 10 metaphases per sample was quantified using TFL-Telo software (kind gift from P. Lansdorp, Vancouver, BC).

Karyotypic analyses

Between 50 and 100 metaphases were scored for chromosomal aberrations in each cell preparation. Aberrations were classified into chromosome type (acentrics, centrics, dicentrics, rings, chromosome breaks, and chromosome fusions) and chromatid type (chromatid breaks, chromatid fusions). Chromosome and chromatid fusions were further classified as either with telomeric signal present at the fusion point or with no telomeric signal at the fusion point.

Chromosome breakage assay

Splenocytes were grown on 10% fetal calf serum (FCS)/RPMI supplemented with concanavalin A (5 μg/mL) (T cells) or lipopolysaccharide (LPS) (10 μg/mL) (B cells). BMCs were grown in Myelocult supplemented with interleukin-3 (IL-3). After 24 hours of culture, MMC (10 or 40 ng/mL) was added for 48 hours.[40] Primary or 3T3-immortalized MEFs were grown in 10% FCS/Dulbecco modified Eagle medium (DMEM) and exposed to MMC (15 to 250 ng/mL) for 48 hours.[32] Cells were incubated in colcemid 0.1 μg/mL for 2 hours, resuspended in 30 mM sodium citrate, and fixed in methanol/acetic acid following standard procedures. For irradiation studies, exponentially growing cells received either 2 or 4 Gy from a 137-Cesium (^{137}Cs) source 12 hours prior to fixation.[40]

Measurement of telomerase activity (TRAP assay)

S-100 extracts were prepared from different cell types, and a modified version of the telomeric repeat amplification protocol (TRAP) assay was used to measure telomerase activity.[41] An internal control for polymerase chain reaction (PCR) efficiency was included (TRAPeze kit; Oncor, Gaithersburg, MD).

Combined PML and telomeric DNA detection

PML foci were visualized by indirect immunofluorescence of BMCs and splenocyte cytospin preparations. Briefly, cultured cells were spun at 260*g* for 3 minutes onto coated slides, air dried, and fixed in cold 4% paraformaldehyde (PFA) for 20 minutes. After permeabilization in 0.5% Triton-X/PBS and blocking in 10% bovine serum albumin/phosphate-buffered saline (BSA/PBS), slides were incubated with a rabbit anti–promyelocytic leukemia (anti-PML) antibody (kind gift from Paul Freemont, Imperial Cancer Research Foundation [ICRF], London, United Kingdom) overnight at 4°C, washed, and incubated with an FITC-labeled goat anti–rabbit antibody. Slides were mounted in Vectashield containing DAPI (Vector Laboratories, Burlingame, CA) and examined under a fluorescence microscope (Leitz DMRB; Leica). For alternative lengthening of telomeres (ALT)–associated PML body (APB) detection, PML immunofluorescence was carried out as described above, followed by telomeric fluorescence in situ hybridization (FISH) with minor modifications to preserve antibody binding. Slides were examined for colocalization of PML and telomeric DNA using a Leica TCS-NT confocal microscope.

FANCG knock-down by short hairpin RNA interference

Short hairpin RNAs (shRNAs) for human (positions 226, 888, 1327, and 1675) and mouse *Fancg* (positions 945, 1020, 1443, and 1518) were ligated with pSUPER.retro (OligoEngine, Seattle, WA) as described,[42] and 15 μg of each plasmid was transfected into 293T cells by the calcium phosphate

coprecipitation method. Retroviral supernatants were filtered and incubated with target cells (either passage 1 [P1] MEFs or IMR90 cells) in the presence of polybrene 8 μg/mL. After puromycin selection, the extent of interference was assessed by real-time reverse transcriptase (RT)–PCR of target cell cDNA. Briefly, target cell RNA (RNA Wiz; Ambion, Austin, TX) was incubated with RQ1 RNAse-free DNAse (Promega, Madison, WI) for 30 minutes at 37°C and then reverse transcribed using Superscript II (Life Technologies, Rockville, MD), following manufacturer's instructions. Real-time RT-PCR was performed in an ABI PRISM 77 000 instrument (Applied Biosystems, Foster City, CA) using SYBR Green PCR Core Reagents (Applied Biosystems). Quadruplicates of serial cDNA 10-fold dilutions were used for both *Fancg* and *β-actin,* and relative *Fancg* expression was adjusted by calculating $\Delta\Delta C_t$ values, which express the difference between the cycle threshold of the *Fancg* primer pair and that of the β-actin mRNA primer pair. All PCRs were repeated at least twice. The following primers were used: mouse *Fancg*: 5′-CCCAAAATGTCCTCCTTGTGG G-3′ (sense) and 5′-AGTGCCACGTCAGACCTACACT-3′ (antisense); human *FANCG*: 5′-GGATGCCCAGGGATTGAAGGAT-3′ (sense) and 5′-GGGCTGCAACCAAGTACAACA G-3′ (antisense); *β-actin* (mouse and human): 5′-GGCACCACACCTTCTACAATG-3′ (sense) and 5′-GTGGTGGTGAAGCTGTAG-3′ (antisense).

Immunoprecipitation and immunoblotting

Exponentially growing cells (10 million) were resuspended in lysis buffer (50 mM Tris [tris(hydroxymethyl)aminomethane] pH 7.4, 150 mM NaCl, 1% Nonidet P-40 [NP-40]) supplemented with protease inhibitors. Fancg was immunoprecipitated with antibody GP-3 (5 μL).[33] For Fancg detection on Western blots, antibody Rb3920 was used (1:1000 dilution).

Results

Telomere length maintenance in *Fancg*$^{-/-}$ hematopoietic cells

Telomere length in fresh BMCs and splenocytes derived from Fancg-deficient mice and wild-type littermates was compared using independent techniques. First, we used Southern blot analysis to determine the size of the so-called terminal restriction fragments (TRFs), which are indicative of the length of TTAGGG repeats at telomeres (see "Materials and methods"). TRFs did not differ significantly in size between genotypes (Figure 1A), suggesting a normal telomere length in Fancg-deficient mice. Next, we used combined flow cytometry and FISH with an FITC-labeled telomeric PNA probe (flow-FISH; see "Materials and methods") to determine telomere fluorescence of G_0/G_1-gated cells (Figure 1B; see "Materials and methods"). Again, average telomere fluorescence was similar in *Fancg*$^{-/-}$ and wild-type cells. Finally, to measure the length of individual telomeres, we used quantitative telomeric FISH (Q-FISH) on metaphase spreads from bone marrow cells and splenocytes. Quantification of individual telomere fluorescence on metaphase chromosomes also indicated that average telomere length was not affected in the absence of Fancg in 2 litters (Figure 1C). More important, the distribution of individual telomere lengths was similar in both genotypes, indicating that the *Fancg*$^{-/-}$ cells did not have a population of critically short telomeres (Figure 1C).

Normal-length telomeres, however, may still fail to cap chromosome ends efficiently,[43] leading to inappropriate joining to other broken ends.[44] To assess capping function in *Fancg*$^{-/-}$ cells, we performed the quantitative telomeric FISH assay on metaphase preparations from mitogen-stimulated BMCs and splenocytes to determine the involvement of telomeres in spontaneous chromosomal aberrations. Neither chromosome ends without detectable telomeric signal (Figure 1C) nor end-to-end fusions were present in *Fancg*$^{-/-}$ metaphases (Table 1 and Supplementary Table 1) (at the *Blood* website, see the Supplemental Materials link at the top of the online article), indicating that telomere capping was preserved in mouse hematopoietic cells in the absence of *Fancg*. Because the rate of spontaneous aberrations in *Fancg*$^{-/-}$ cultures is rather low (Yang et al[40] and our own observations), we also performed Q-FISH assay on metaphases from *Fancg*$^{-/-}$ BMCs and splenocytes after treatment with the clastogen mitomycin C (MMC) at doses of 10 and 40 ng/mL.[41] Chromatid breaks and chromatid fusions involving 2 or more chromosomes were typically observed, as well as occasional secondary aberrations, to a higher frequency in Fancg-deficient cells than in wild-type controls (Supplementary Figure 1; Supplementary Table 1). Because telomeric FISH allows

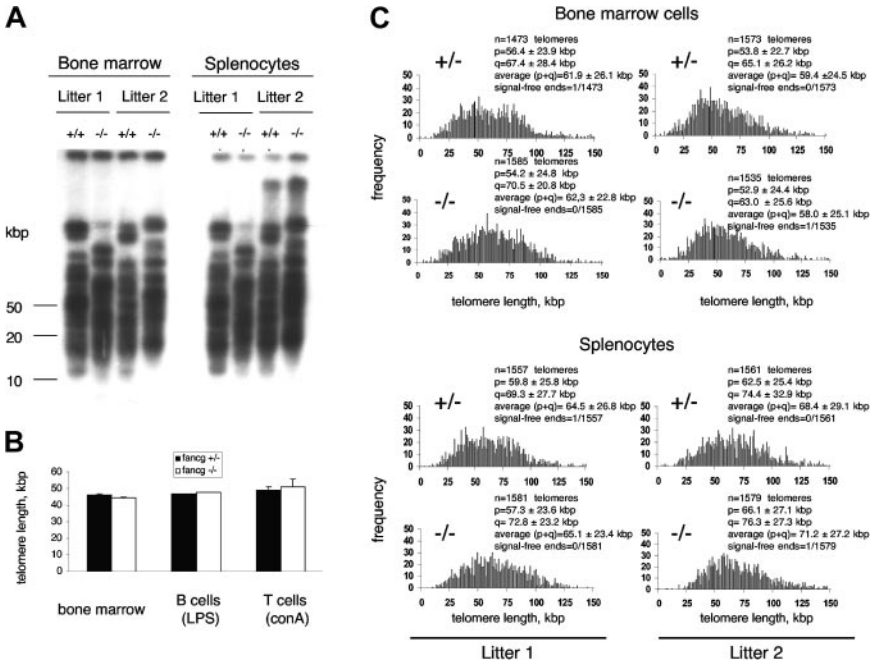

Figure 1. Telomere maintenance in *Fancg*$^{-/-}$ hematopoietic cells. (A) Telomere restriction fragments of BMCs and concanavalin A–stimulated splenocytes. Note the absence of telomeric signals below 10 kbp and similar TRF distribution in all genotypes. (B) Comparative telomere length of G_0/G_1 hematopoietic cells by flow-FISH analysis. Mean and standard deviation of results from 2 mice per group are shown. (C) Comparison of telomere length average and distribution of *Fancg*$^{-/-}$ BMCs and splenocytes and their *Fancg*$^{+/-}$ littermates. Ten metaphases per mouse were analyzed after hybridization with a Cy3-labeled telomere-specific PNA probe.

Table 1. Detection of TTAGGG repeats in chromatid breaks and fusions in clastogen-treated *Fancg*$^{-/-}$ cells by Q- FISH analysis

Treatment	Chromatid breaks		Chromatid fusions	
	With TTAGGG at the break	Without TTAGGG at the break	With TTAGGG at the fusion point	Without TTAGGG at the fusion point
Clastogen				
Splenocytes				
Nontreated	0	0.3	0	0
MMC, 10 ng/mL	0	3.9	0	0.05
MEFs				
Nontreated	0	0.07	0	0
MMC, 15 ng/mL	0	1.4	0	0.53
γ-irradiation				
Splenocytes				
Nontreated	0	0.1	0	0
2 Gy	0	0.38	0	0.03
4 Gy	0	0.38	0	0.08
BMCs				
Nontreated	0	0.1	0	0
2 Gy	0	0.1	0	0
4 Gy	0	0.92	0	0.36
MEFs				
Nontreated	0	0.06	0	0
2 Gy	0	0.23	0	0.08

All numbers are aberrations per metaphase.

for visualization of all individual telomeres, we examined the ends of broken chromosomes and the fusion points to determine the frequency of telomere rejoining to breaks in Fancg-deficient cells, which is diagnostic of telomere dysfunction. Significantly, we observed that chromatid breaks remained uncapped and no acquisition of new telomeres was observed (Table 1), in agreement with a normal telomere capping function in *Fancg*$^{-/-}$ cells. Furthermore, chromatid fusions invariably lacked telomeric signals at the fusion point, indicating that telomeres did not participate in rejoining with DNA breaks (Table 1). In addition, chromosome-type aberrations (dicentrics, centric and acentric chromosomes, and rings) were elicited by exposing *Fancg*$^{-/-}$ splenocytes and BMCs to γ-radiation (2 Gy and 4 Gy; Supplementary Figure 1; Supplementary Table 1). However, Q-FISH analysis of metaphase preparations from irradiated cells showed that, like wild-type telomeres, *Fancg*$^{-/-}$ telomeres were not involved in fusions with DNA breaks in this setting either (Table 1).

Telomerase activity maintains telomere length in *Fancg*$^{-/-}$ hematopoietic cells

Normal somatic and germ cells maintain telomeres by telomerase activation.[45] A telomerase-independent recombination-based mechanism for alternative lengthening of telomeres (ALT) has also been described.[46] ALT cells typically show marked heterogeneity in telomere length and no detectable telomerase activity. ALT-associated PML bodies (APBs) are nuclear foci–containing PML, telomeric DNA, and telomeric proteins and are considered pathognomonic of ALT in mammalian cells.[46]

To investigate mechanisms of telomere maintenance in the absence of Fancg, we first compared telomerase activity in *Fancg*$^{-/-}$ and *Fancg*$^{+/+}$ lymphocyte and BMC cultures. *Fancg*$^{-/-}$ lymphocytes up-regulated telomerase in response to specific mitogens to a similar degree as their Fancg$^{+/+}$ counterparts (Supplementary Figure 2A). In addition, no telomerase activity was detected in either *Fancg*$^{+/+}$ or *Fancg*$^{-/-}$ BMCs that had been grown in interleukin-3–enriched media for 72 hours, indicating that down-regulation of telomerase activity with differentiation is also adequate in Fancg-deficient cells (not shown).

We next examined *Fancg*$^{-/-}$ splenocytes and BMCs for the presence of APBs in order to exclude ALT activation in the absence of Fancg. In particular, FANCG has been linked to HR by its interaction with BRCA2 [31] and the inability of FANCG-deficient cells to repair classical double-strand breaks (DSBs) by HR in some experimental systems.[47] Using indirect immunofluorescence, we detected no difference in the number and distribution of PML nuclear foci in *Fancg*$^{-/-}$ and *Fancg*$^{+/-}$ cells (Supplementary Figure 2B). Furthermore, combined immunofluorescence to PML followed by Q-FISH for telomere detection failed to detect colocalization of telomeric DNA and PML (Supplementary Figure 2C). These observations, together with the lack of changes in telomere length distribution (Figure 1C) and the normal levels of telomerase (Supplementary Figure 2A), suggest that, like for wild-type cells, telomerase activity is responsible for telomere maintenance in *Fancg*$^{-/-}$ hematopoietic cells.

Telomere maintenance in purified *Fancg*$^{-/-}$ hematopoietic stem cells and progenitors

Fancg mRNA is highly expressed in purified Lin$^-$Thy1.2$^-$ hematopoietic stem cells.[48] Using Fancg$^{-/-}$ mice as a model, multiple defects at the stem and precursor cell compartments have been characterized, including decreased repopulation potential,[49,50] a defect in stem cell cycling,[51] and increased sensitivity to nitric oxide.[52] However, these defects do not result in spontaneous bone marrow failure, indicating that, unlike human beings, mice can compensate for defective stem/precursor cell dysfunction, perhaps related to their longer telomeres. To study telomere function at earlier stages of hematopoietic development, we obtained populations of whole bone marrow, low-density mononuclear cells (LDMNCs), and Lin$^-$ cells (estimated enrichment in stem cells, 100-fold) from 3 pairs of Fancg-proficient and -deficient female littermates for comparative telomere analysis. Similar to previous results, telomere restriction fragments (TRFs) of whole bone marrow cells or LDMNCs did not differ significantly between genotypes; nor did TRFs of pooled *Fancg*$^{+/+}$ and *Fancg*$^{-/-}$ Lin$^-$ cells (pool of 3 mice per genotype; Figure 2A). Furthermore, measurement of individual telomeres by quantitative telomeric FISH revealed significant differences in telomere length according to the stem cell content but not to genotype. Thus, for wild-type cells, average telomere length of pooled (n = 3) LDBMCs and Lin$^{-/-}$ cells was 56.4 ± 22.7 and 61.6 ± 25.1 kbp, respectively. Similarly, average telomere length of Fancg-deficient pooled (n = 3) LDBMCs and Lin$^{-/-}$ cells was 60.3 ± 22.8 and 63.2 ± 25.4 kbp, respectively (Figure 2B). The loss of 3 to 5 kbp in the more differentiated cells of either genotype compared with the Lin$^-$ population purified from the same mice is in agreement with previously published reports indicating that telomerase up-regulation in the highly proliferative stem and precursor cell compartment is not sufficient to fully compensate for replication-associated telomere loss in the hematopoietic system.[53] To study whether telomere shortening with hematopoietic cell differentiation was homogeneous at all telomeres independent of their length, we calculated telomere length differences (Δtelomere length) between Lin$^-$ and LDMNCs for the 10th, 25th, 50th, 75th, and 90th percentiles in both wild-type and Fancg-deficient cells. At all percentiles, telomeres were longer in Lin$^-$ cells compared with LDMNCs of the same genotype; the absolute telomere length difference (Δtelomere length) in kbp is shown in Figure 2C.

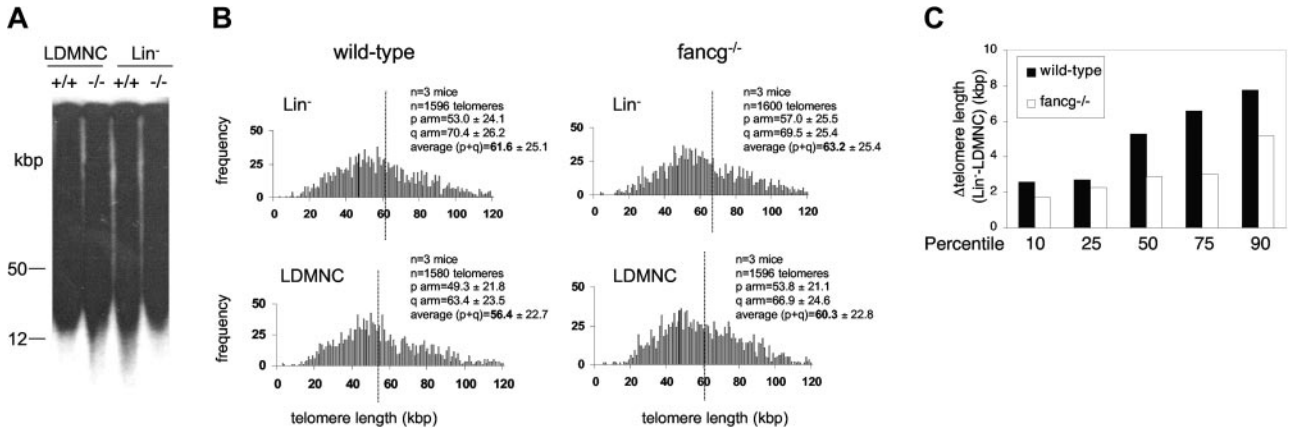

Figure 2. Telomere maintenance in purified stem cell–enriched *Fancg*$^{-/-}$ hematopoietic cells. (A) Telomere restriction fragments (TRFs) of hematopoietic cell populations progressively enriched for stem cells. Pooled low-density mononuclear cells (LDMNCs) were obtained (3 per genotype), and Lin$^-$ cells were isolated from the pooled cells and run on the same blot for comparison. Loading, 50 000 cells per lane. (B) Q-FISH analysis of pooled LDMNCs and Lin$^{-/-}$ wild-type and *Fancg*$^{-/-}$. The average telomere length for each histogram is shown as a vertical line; deviation to the right in the Lin$^{-/-}$ populations of both genotypes indicates increased telomere reserve compared with the more differentiated LDMNCs. (C) To study whether telomere shortening with differentiation was homogeneous in all telomeres independent of their length, we calculated telomere length differences (Δtelomere length) between Lin$^-$ and LDMNCs for the 10th, 25th, 50th, 75th, and 90th percentiles. Although telomeres were longer in the Lin$^-$ population at all percentiles and independent of the genotype, telomere loss with differentiation was significantly greater in the higher percentiles compared with the lower, indicating preferential maintenance of short telomeres with differentiation in both wild-type and *Fancg*$^{-/-}$ cells.

Significantly, for wild-type cells, the 10th percentile was 30.9 kbp for Lin$^-$ cells and 28.3 kbp for LDMNCs (Δtelomere length (Lin$^-$ − LDMNCs) = 2.6 kbp), while the 90th percentile for the same cells was 97.0 kbp and 89.3 kbp (Δtelomere length (Lin$^-$ − LDMNCs) = 7.3 kbp) (Figure 2C), indicating that the overall shift to the left in the histogram of the more differentiated cells (Figure 2B) was accompanied by a selective loss of long telomeres. This finding is in agreement with prior observations indicating that telomerase acts preferentially on the shortest telomeres in the cell.[54,55] Similarly, comparison of the 10th and 90th percentiles of telomere length in *Fancg*$^{-/-}$ populations revealed a 2.9-kb telomere loss at the 10th percentile (from 63.2 kbp in Lin$^-$ cells to 60.3 kbp in LDMNCs) and a 5.2 kbp loss at the 90th percentile (from 96.7 kbp in Lin$^-$ cells to 91.5 kbp in LDMNCs) similar to that found for wild-type cells (Figure 2C). Therefore, although telomeres were longer in the Lin$^-$ population at all percentiles, telomere loss with differentiation was significantly greater in the higher percentiles compared with the lower, indicating preferential maintenance of short telomeres with differentiation in both wild-type and *Fancg*$^{-/-}$ cells. The similar behavior of wild-type and *Fancg*-deficient cells suggests that the preferential elongation of short telomeres by telomerase is not altered in the absence of Fancg.

Cytogenetic analysis of wild-type and *Fancg*$^{-/-}$ pooled LDBMCs and Lin$^{-/-}$ cells revealed normal euploid karyotypes, detectable telomeric signals in all chromosome ends, and no end-capping defects, as shown by the absence of end-to-end chromosomal fusions (data not shown). Overall, our data suggest normal telomere reserve in a more primitive hematopoietic compartment (Lin$^-$ cells) and appropriate rate of telomere loss with proliferation and differentiation in *Fancg*$^{-/-}$ hematopoietic precursors.

Telomere dynamics in nonhematopoietic *Fancg*$^{-/-}$ tissues

Compromised primordial germ cell proliferation and adult germ cell degeneration, leading to tubular atrophy and male infertility, has been described in all mouse models of FA generated to date.[21] Although the molecular basis of germ cell degeneration is not well understood, chromosome miss-pairing during meiotic prophase 1 is a prominent feature of Fanconi-deficient meiocytes, and few progress past this stage.[56,57] Because meiotic telomeres are key elements in progression through prophase 1,[58] we investigated whether abnormal telomere maintenance in the absence of Fancg contributed to germ cell degeneration. Quantification of individual telomeric signals in pachytene cells of paraffin-embedded testis sections stained with a telomere-specific PNA probe (Supplementary Figure 3A-C) revealed no differences between genotypes. In fact, telomere fluorescence of *Fancg*$^{-/-}$ pachytene cells in tubules where meiotic function was preserved and in adjacent tubules showing extensive degeneration did not differ significantly (Supplementary Figure 3C-D for examples; Supplementary Figure 3E for quantification). Furthermore, telomere restriction fragments of nuclei suspensions of adult testis (high Fancg expression) and liver and kidney (no Fancg expression) were obtained for measurement of telomere restriction fragments; no differences in molecular weight or fragment distribution were observed (Supplementary Figure 3F). Similarly, telomerase activity was present in the testis (reflecting activation in cycling spermatogonia) and in the liver of *Fancg*$^{-/-}$ extracts to comparable degree to their wild-type littermates (Supplementary Figure 3G). These results argue against a specific defect in telomerase activation or addition of telomeric repeats in *Fancg*$^{-/-}$ spermatogonia or a telomere-mediated impairment in chromosomal alignment during prophase I.

We also analyzed telomere dynamics of primary wild-type and *Fancg*$^{-/-}$ mouse embryonic fibroblasts (MEFs). We found no significant difference in telomere length between *Fancg*$^{+/+}$ and *Fancg*$^{-/-}$ MEFs using either the TRF assay (Supplementary Figure 4A) or the Q-FISH assay (Supplementary Figure 4B). Furthermore, treatment of MEFs with MMC or γ-radiation elicited a dose-dependent increase in genomic instability (Supplementary Figure 1) but no concomitant loss of telomere capping function (Supplementary Figure 4C-J; Table 1). Finally, telomerase activity was detectable in passage 2 MEFs of both *Fancg*$^{+/+}$ and *Fancg*$^{-/-}$ genotypes (Supplementary Figure 4K).

Telomere dynamics in Fancg knock-down telomerase-deficient cells with human lengthlike telomeres (G5 *Terc*$^{-/-}$*/Fancg* shRNA3 MEFs)

Telomeres of inbred mice are significantly longer than human telomeres,[38] which raises the issue of whether the lack of aplastic anemia in Fancg-deficient mice and of a telomeric defect (Figure 2)

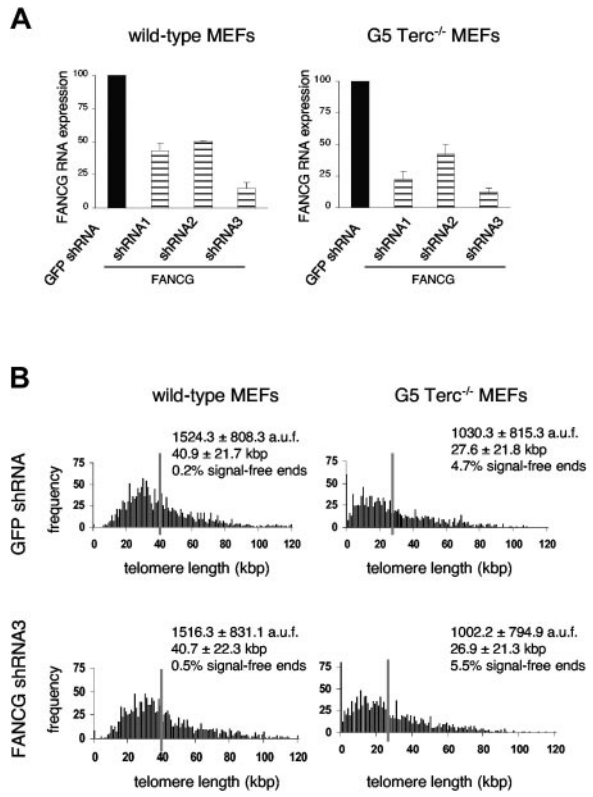

Figure 3. Telomere dynamics in Fancg knock-down primary MEFs with humanlike telomere length (G5 *Terc*$^{-/-}$*/Fancg* shRNA3 MEFs). (A) Specific *Fancg* RNA interference was measured by real-time RT-PCR 7 days after infection of P3 wild-type or G5 *Terc*$^{-/-}$ MEFs with retroviruses encoding *Fancg* shRNAs; relative values to a control *GFP* shRNA are shown. Bars represent average and standard deviation of 2 independent assays. (B) Q-FISH analysis of P3 MEFs 7 days after infection with retroviruses expressing either GFP shRNA or *Fancg* shRNA3. Most significantly, average telomere length, length distribution, and frequency of signal-free ends were unchanged in G5 *Terc*$^{-/-}$*/Fancg* shRNA3 MEFs (bottom right panel) compared with their G5 *Terc*$^{-/-}$*/GFP* shRNA controls (top right panel) despite nearly 90% inhibition of *Fancg* expression.

could relate to their greater telomere reserve. To investigate the effect of Fancg depletion on mouse cells with humanlike telomere length, we infected passage 1 (P1) telomerase-deficient fifth-generation (G5) Terc$^{-/-}$ MEFs with critically short telomeres with 4 retroviral constructs expressing *Fancg* shRNAs using the pSUPER.retro system (see "Materials and methods"). As shown in Figure 3A, 3 of 4 tested shRNAs induced the degradation of more than 50% of *Fancg* mRNA, compared with a control green fluorescent protein *(GFP)* shRNA. In particular, Fancg shRNA3 induced a 10-fold decrease in *Fancg* mRNA expression (14.6% ± 4.8% and 11.9% ± 3.4% of the GFP shRNA control at day 7 after infection in wild-type and G5 *Terc*$^{-/-}$ MEFs, respectively; Figure 3A; Table 2) and was used for Q-FISH analysis of individual telomeres on metaphases spreads (Figure 3B). Thus, average telomere length was 40.7 ± 22.3 kbp for *Terc*$^{+/+}$*/GFP* shRNA MEF and 40.9 ± 21.7 kbp for *Terc*$^{+/+}$*/Fancg* shRNA3 MEFs (Figure 3B; Table 2), in agreement with our observations in *Fancg*$^{-/-}$ MEFs (Supplementary Figure 4B). As expected, G5 *Terc*$^{-/-}$/GFP shRNA MEFs showed significantly shorter telomeres (27.3 ± 21.8 kbp), with an increased number of signal-free ends (4.7% of chromosome ends) and a mild increase in Robertsonian-like chromosomal fusions (0.08 fusions per metaphase), which are all hallmarks of telomere dysfunction (Figure 3B; Table 2). Significantly, comparative analysis of G5 *Terc*$^{-/-}$*/Fancg* shRNA3 MEFs revealed similar telomere length (26.9 ± 21.3) and frequency of signal-free ends (5.5%) and a slight increase in fusions (0.2 fusions per metaphase) (Figure 3B; Table 2), suggesting that the lack of a telomere-related phenotype observed in Fancg-deficient mice is not due to their longer telomeres but rather to telomere maintenance being *Fancg*-independent in nature.

Telomere dynamics in immortalized Fancg knock-down cells (immortal G5 *Terc*$^{-/-}$*/Fancg* shRNA3 MEFs)

Telomerase-deficient G5 *Terc*$^{-/-}$ MEFs can be immortalized in culture, most likely thanks to the activation of ALT mechanisms.[36,39] To investigate whether *Fancg*, which supports HR,[47] plays a role in ALT initiation or maintenance, we subjected *Terc*$^{+/+}$*/Fancg* shRNA3 and G5 *Terc*$^{-/-}$*/Fancg* shRNA3 cells and their respective *GFP* shRNA controls to a standard 3T3 protocol. All MEF cultures immortalized at approximately the same time interval (data not shown), and the extent of *Fancg* RNA interference in the immortal cell lines, determined by real-time RT-PCR, was similar to their primary counterparts (Figure 4A; Table 2). Moreover, Fancg immunoprecipitation and Western blotting (IP/WB) revealed marked inhibition of protein synthesis (Figure 4B), indicating that our measurements of *Fancg* RNA expression by real-time RT-PCR are reliable indicators of protein expression. Using Q-FISH analysis, we found that telomere length was 21.8 ± 20.3 kbp and 23.8 ± 22.2 kbp in immortalized G5 *Terc*$^{-/-}$*/GFP* shRNA and G5 *Terc*$^{-/-}$*/Fancg* shRNA3 MEFs, respectively, a similar reduction of 5.8 and 3.2 kbp from the parental primary cultures (Figure 4C; Table 2). In addition, the number of signal-free ends and end-to-end fusions, which is increased in immortalized late-generation telomerase-deficient cells,[34] was similarly increased in both (Figure 4C; Table 2), indicating that most Fancg is

Table 2. Telomere dynamics of FANCG knock-down wild-type and G5 *Terc*$^{-/-}$ MEFs

Genotype	shRNA (%RNA)*	Telomere length a.u.f. (kbp)	Signal-free ends, %	RT-like fusions per metaphase
Primary MEFs				
Wild-type	GFP shRNA (100)	1516.3 ± 831.1 (40.7 ± 22.3)	0.5	0
	FANCG shRNA3 (14.6 ± 4.8)	1524.3 ± 808.3 (40.9 ± 21.7)	0.2	0
G5 Terc$^{-/-}$	GFP shRNA (100)	1030.3 ± 815.3 (27.6 ± 21.8)	4.7	0.08
	FANCG shRNA3 (11.9 ± 3.4)	1002.2 ± 794.9 (26.9 ± 21.3)	5.5	0.2
Immortalized MEFs				
Wild-type	GFP shRNA (100)	1656.7 ± 916.0 (44.4 ± 24.5)	0.8	0
	FANCG shRNA3 (30.2 ± 4.2)	1456.7 ± 847.5 (39.1 ± 22.7)	0.8	0
G5 Terc$^{-/-}$	GFP shRNA (100)	814.3 ± 757.1 (21.8 ± 20.3)	10.3	4.88
	FANCG shRNA3 (16.2 ± 1.1)	889.2 ± 829.2 (23.8 ± 22.2)	12.1	3.93

a.u.f. indicates arbitrary units of fluorescence.

*Average and standard deviation of 2 independent real-time RT-PCR assays; MEFs of the same genotype assayed in parallel are considered as 100% *FANCG* RNA.

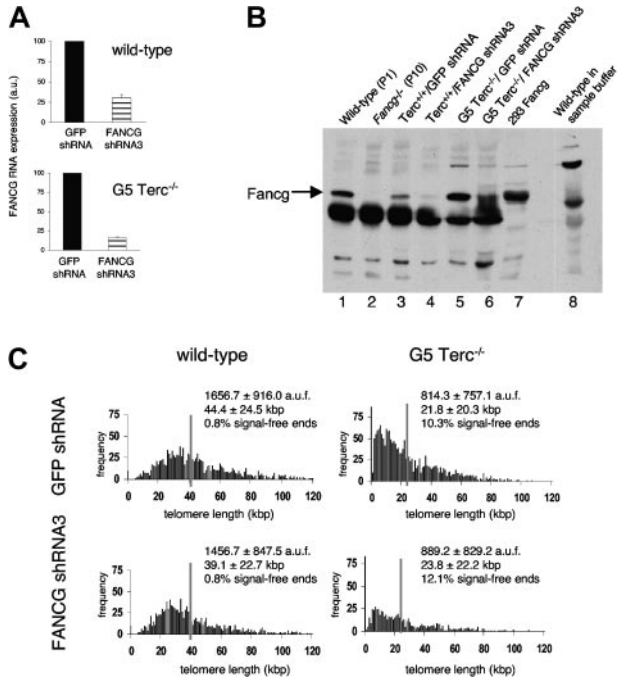

Figure 4. Fancg knock-down in immortalized telomerase-deficient mouse cells with humanlike telomere length (G5 *Terc*$^{-/-}$*/Fancg* shRNA3 MEFs). (A) GFP shRNA and *Fancg* shRNA3 MEFs in wild-type and G5 *Terc*$^{-/-}$ backgrounds were immortalized following a 3T3 protocol, and specific *Fancg* interference was assessed by real-time RT-PCR. Extent of interference was similar to primary MEFs. (B) Correlation between RNA interference and protein knock-down was assessed by IP and Western blot. Fancg expression is readily detected in wild-type MEFs and 293 cells transfected with a Fancg vector (lanes 1 and 7, respectively) and absent in *Fancg*$^{-/-}$ MEFs (lane 2). Significantly decreased protein expression is observed in *Terc*$^{+/+}$/*Fancg* shRNA3 MEFs (lane 4) compared with their *Terc*$^{+/+}$/*GFP* shRNA controls (lane 3) and in G5 *Terc*$^{-/-}$/*Fancg* shRNA3 MEFs (lane 6) compared with their G5 *Terc*$^{-/-}$/*GFP* shRNA controls (lane 5). (C) Q-FISH analysis of immortalized *Terc*$^{+/+}$/*Fancg* shRNA3 and G5 *Terc*$^{-/-}$/*Fancg* shRNA3 MEFs and their *GFP* shRNA-expressing controls. Like G5 *Terc*$^{-/-}$/*GFP* shRNA control telomeres, G5 *Terc*$^{-/-}$/*Fancg* shRNA3 telomeres showed very heterogeneous telomere length and frequent signal-free ends, indicative of ALT activation in these cells with critically short telomeres and no telomerase activity.

dispensable for telomere maintenance and growth in the absence of telomerase activity.

Telomere dynamics in FANCG-deficient human cells

An alternative explanation for the differences observed in Fancg-deficient mouse and human cells (ie, the lack of aplastic anemia in the former) could relate to differential roles of FANCG in the 2 species, although this seems unlikely in face of the functional complementation of mouse and human proteins.[33] To solve this issue, we evaluated telomere dynamics directly in FANCG-deficient human metaphases. To this end, we infected late-passage IMR90 cells expressing the ecotropic receptor with retroviral constructs encoding for 4 specific human *FANCG* shRNAs or a control *GFP* shRNA (see "Materials and methods"). On day 10 after infection, *FANCG* RNA expression was assessed by real-time RT-PCR; *FANCG* shRNA2 achieved the best interference (40% ± 6.6% of the *GFP* control; data not shown) and was used for telomere studies. Average telomere length at day 10 after infection was 4.9 ± 3.6 kbp and 4.9 ± 3.6 kbp for *GFP* shRNA and *FANCG* shRNA2 IMR90 cells, respectively (Figure 5A), in agreement with our previous results in Fancg knock-down mouse cells.

Because residual FANCG expression could mask a role of FANCG in telomere maintenance in this system, we also obtained metaphase spreads from 2 independent early-passage primary fibroblast cultures from 2 patients of the complementation group G. As shown in Figure 5B, mean telomere length was 10.5 ± 4.2 kbp and 9.7 ± 5.2 kbp in primary skin fibroblasts from one 4-year-old and one 16-year-old FA group G patients, respectively. These values are reportedly in the normal range for age.[59] More important, telomere length distribution was homogeneous (compare normal distribution of the histograms in Figure 5B with marked left shift in late-passage IMR90 histograms in Figure 5A), and the number of chromosome ends without detectable telomeric signal was low, as previously reported for early-passage normal fibroblasts cultures.[60] Similarly, we did not detect increased end-to-end telomere fusions in these cells, which could be indicative of

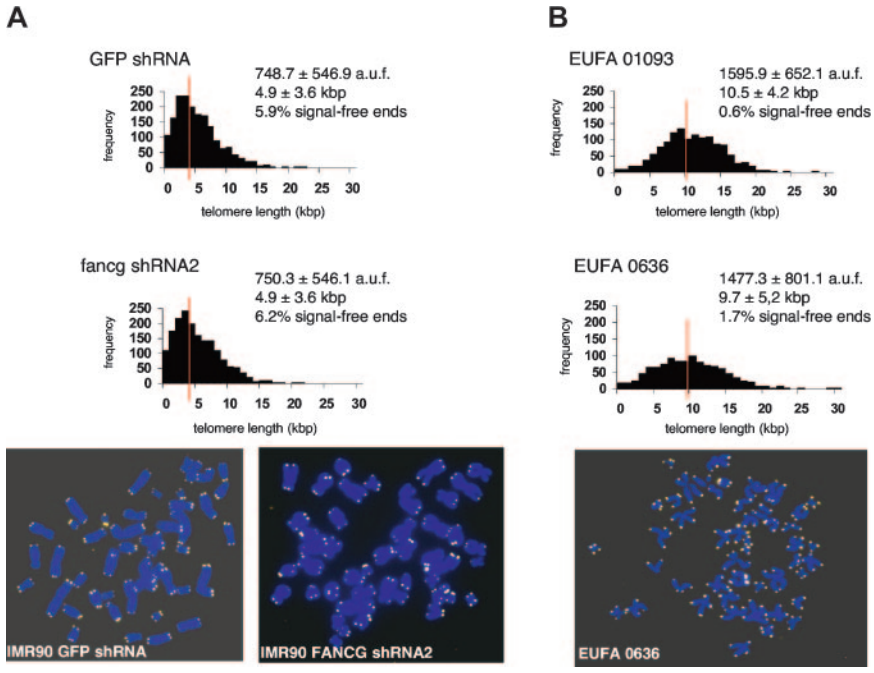

Figure 5. Telomere dynamics in FANCG-deficient human cells. (A) Q-FISH analysis of presenescent IMR90 cells infected with retrovirus encoding *FANCG* shRNAs or *GFP* shRNA, at day 10 after infection. Histograms show similar telomere length distribution in *GFP* shRNA IMR90 cells and *FANCG* shRNA2 IMR90 cells (top 2 panels). Representative microphotographs (telomeric probe, yellow; DNA, blue) are shown in the bottom 2 panels. (B) Telomere length distribution of early-passage primary fibroblasts (CPD5) obtained from 2 FA-G patients (EUFA 1093-F and EUFA 0636). Note the very homogeneous telomere length and absence of signal-free ends or end-to-end chromosomal fusions. A representative microphotograph of a metaphase from patient EUFA 0636 is shown in the bottom panel.

telomeric dysfunction (not shown). Interestingly, when we measured in parallel telomere length in primary skin fibroblasts from a 4-year-old healthy donor that had been extensively passaged in culture (CD15), these cells showed decreased average telomere length and marked increase in the number of signal-free ends (data not shown) compared with the 4-year-old and 16-year-old FA group G patients. Together these results suggest that replicative history and/or accumulated metabolic stress may be the main determinant of telomere loss in human Fancg-deficient fibroblasts, as previously suggested by others.[26]

Discussion

We undertook this study to clarify whether the accelerated telomere shortening previously reported in hematopoietic cells of patients with FA was due to a primary telomeric defect (ie, the FA pathway is required for telomere metabolism) or was secondary (ie, due to the increased cell death and oxidative damage observed in this disorder). This distinction is important in order to establish a rational basis for development of FA aplastic anemia prophylaxis and therapy. We clearly demonstrate here that FANCG, an essential component of the FA nuclear core complex, is dispensable for telomere maintenance in a wide range of mouse and human primary cells with null or severely reduced FANCG expression and specifically in those most affected by the disease (the hematopoietic system, the gonads, and the embryonic tissues).

Telomere dysfunction accelerates disease progression and malignant transformation in many hematologic conditions, probably through a negative effect on genomic instability.[61] However, the mechanisms leading to telomere dysfunction itself are not clearly established for most hematologic diseases. Dyskeratosis congenita (DC), a syndrome of bone marrow aplasia and increased cancer predisposition, is an exception to this; mutations in either the telomerase RNA component or an auxiliary protein, dyskerin, lead to a specific defect in telomere maintenance and to very short dysfunctional telomeres at the onset of marrow aplasia.[62] In contrast, the mechanism underlying telomere dysfunction in FA is not known despite the fact that telomere dysfunction has proved to correlate with disease outcome.[28] Our data and prior work[24-28] could be reconciled in a model of "secondary telomere damage" in FA. In particular, an inverse relationship between cell turnover and telomere length has been shown for hematopoietic cells.[63,64] Moreover, some of the Fanconi proteins possess redox regulatory functions,[65,66] and their absence results in increased DNA oxidation, which has been linked to single-strand breaks at telomeric sites and increased telomere attrition.[67] Therefore, the progressive loss of telomere reserve in FA could be due to increased cell death, deregulated cell cycling, and increased oxidative damage. The fact that Fancg-deficient mice show normal telomere length and function while patients with FA show short dysfunctional telomeres could be at the base of the phenotypic differences between human beings and mice. In this regard, our observations of no additional telomere phenotypes in telomerase-deficient MEFs with "human-like" telomere length with marked reduction of Fancg expression (G5 *Terc*$^{-/-}$*/Fancg* shRNA3 MEFs) strongly suggest that long telomeres in *Fancg*$^{-/-}$ mice are not masking a telomeric role for this protein. However, definitive proof warrants the generation of mice doubly deficient in telomerase and Fancg in order to model the effect of embryogenesis and life-long hematopoiesis on human telomere maintenance in vivo.

Additionally, the generation of a cell line from G5 *Terc*$^{-/-}$*/Fancg* shRNA MEFs, which are obligate ALT users for immortalization, indicates that most Fancg is dispensable for recombination mediated-telomere synthesis, although we cannot exclude that residual Fancg activity in our system is sufficient to mediate this process.

Interestingly, recent data suggest that both FANCD1/BRCA2 and FANCD2 are likely to have downstream functions independent of the FANCG-containing FA core complex,[23] which could include telomere metabolism. In support of this notion, and unlike Fancg mice, Fancd2-deficient mice show epithelial cancers and severe germ cell demise,[57] and FANCD2 has been localized at meitoic telomeres.[68] In the same line, FA-D1 patients show more severe chromosomal instability and early-onset solid tumors than patients of the complementation group G.[69] These observations warrant future studies on the role of other components of the Fanconi anemia pathway at the telomere.

Finally, our finding that Fancg does not have a direct role at telomeres has important consequences for the design of aplasia prevention and therapy in patients with FA of complementation group G, which constitutes 10% of the FA population, and perhaps other complementation groups. While bone marrow transplantation is curative in many patients, the procedure-associated risks increase with HLA mismatch or in patients with advanced disease. Regulated transient expression of telomerase in hematopoietic compartments could delay the onset of telomere dysfunction and potentially provide an alternative to grafting or allow for temporary functional recovery in selected patients. Lastly, further exploring the role of FA proteins at the telomere will contribute to our understanding of how inactivation of this pathway contributes to tumorigenesis in nonsyndromic cancers as well.[70]

Acknowledgment

We thank M. A. D. Berns for tissue culture assistance.

References

1. Blackburn EH. Switching and signalling at the telomere. Cell. 2001;106:661-673.
2. de Lange T. Protection of mammalian telomeres. Oncogene. 2002;21:532-540.
3. Bailey SM, Meyne J, Chen DJ, et al. DNA double-strand break repair proteins are required to cap the ends of mammalian chromosomes. Proc Natl Acad Sci U S A. 1999;96:14899-14904.
4. Hsu H-L, Gilley D, Galande SA, et al. Ku acts in a unique way at the mammalian telomere to prevent end joining. Genes Dev. 2000;14:2807-2812.
5. Samper E, Goytisolo F, Slijepcevic P, van Buul P, Blasco MA. Mammalian Ku86 prevents telomeric fusions independently of the length of TTAGGG repeats and the G-strand overhang. EMBO Rep. 2000;1:244-252.
6. Goytisolo F, Samper E, Edmonson S, Taccioli GE, Blasco MA. Absence of DNA-PKcs in mice results in anaphase bridges and in increased telomeric fusions with normal telomere length and G-strand overhang. Mol Cell Biol. 2001;21:3642-3651.
7. d'Adda di Fagagna F, Hande MP, Tong WM, et al. Effects of DNA non-homologous end-joining factors on telomere length and chromosomal stability in mammalian cells. Curr Biol. 2001;11:1192-1196.
8. Espejel S, Franco, S., Rodríguez-Perales, et al. Mammalian Ku86 mediates chromosomal fusions and apoptosis caused by critically short telomeres. EMBO J. 2002;21:2207-2219.
9. Espejel S, Franco S, Sgura A, et al. Functional interaction between DNA-PKcs and telomerase in telomere length maintenance. EMBO J. 2002;21:6275-6287.
10. Jaco I, Muñoz P, Goytisolo F, et al. Role of mammalian Rad54 in telomere length maintenance. Mol Cell Biol. 2003;23:5572-5580.
11. Tarsounas M, Muñoz P, Claas A, et al. Telomere maintenance requires the RAD51D recombination/repair protein. Cell. 2004;117:337-347.
12. Greider CW, Blackburn EH. Identification of a

specific telomere terminal transferase activity in Tetrahymena extracts. Cell. 1985;43:405-413.

13. Broccoli D, Young JW, de Lange T. Telomerase activity in normal and malignant hematopoietic cells. Proc Natl Acad Sci U S A. 1995;92:9082-9086.
14. Mitchell JR, Wood E, Collins K. A telomerase component is defective in human disease dyskeratosis congenita. Nature. 1999;402:551-555.
15. Vulliamy T, Marrone A, Goldman F, et al. The RNA component of telomerase is mutated in autosomal dominant dyskeratosis congenita. Nature. 2001;413:432-434.
16. Samper E, Fernandez P, Eguia R, et al. Long-term repopulating ability of telomerase-deficient murine hematopoietic cells. Blood. 2002;99:2767-2775.
17. Allsop RC, Morin GB, DePinho R, Harley CB, Weissman IL. Telomerase is required to slow telomere shortening and extend replicative lifespan of HSCs during serial transplantation. Blood. 2003;102:517-520.
18. Ball SE, Gibson FM, Rizzo S, et al. Progressive telomere shortening in aplastic anemia. Blood. 1998;91:3582-3592.
19. Brümmendorf T, Maciejewski JP, Mak J, Young NS, Lansdorp PM. Telomere length in leukocyte subpopulations of patients with aplastic anemia. Blood. 2001;15:895-900.
20. Baerlocher GM, Röth A, Lansdorp PM. Telomeres in hematopoietic cells. Ann N Y Acad Sci. 2003; 996:44-48.
21. D'Andrea AD, Grompe M. The Fanconi anaemia/BRCA pathway. Nat Rev Cancer. 2003;3:23-34.
22. Rothfuss A, Grompe M. Repair kinetics of genomic interstrand DNA cross-links: evidence for DNA double-strand break-dependent activation of the Fanconi anemia/BRCA pathway. Mol Cell Biol. 2004;24:123-134.
23. Venkitaraman AR. Tracing the network connecting BRCA and Fanconi anaemia proteins. Nat Rev Cancer. 2004;4:266-276.
24. Leteurtre F, Li X, Guardiola P, et al. Accelerated telomere shortening and telomerase activation in Fanconi's anaemia. Br J Haematol. 1999;105: 883-893.
25. Hanson H, Mathew CG, Docherty Z, et al. Telomere shortening in Fanconi anemia demonstrated by a direct approach. Cytogenet Cell Genet. 2001;93:203-206.
26. Adelfalk C, Lorenz M, Serra V, et al. Accelerated telomere shortening in Fanconi anemia fibroblasts - a longitudinal study. FEBS Lett. 2001; 506:22-26.
27. Callen E, Samper E, Ramirez MJ, et al. Breaks at telomeres and TRF2-independent end fusions in Fanconi anemia. Hum Mol Genet. 2002;11:439-444.
28. Li X, Leteurtre F, Rocha V, Guardiola P, et al. Abnormal telomere metabolism in Fanconi's anemia correlates with genomic instability and the probability of developing severe aplastic anemia. Br J Hematol. 2003;120:836-845.
29. de Winter JP, Waisfisz Q, Rooimans MA, et al. The fanconi anemia group G gene FANCG is identical with XRCC9. Nat Genet. 1998;20:281-283.
30. Blom E, van de Vrugt HJ, de Winter JP, Arwert F, Joenje H. Multiple TPR motifs characterize the Fanconi anemia FANCG protein. DNA Repair. 2004;3:77-84.
31. Hussain S, Witt E, Huber PA, Medhurst AL, Ashworth A, Mathew CG. Direct interaction of the Fanconi anemia protein FANCG with BRCA2/FANCD1. Hum Mol Genet. 2003;12:2503-2510.
32. Koomen M, Cheng NC, van de Vrugt HJ, et al. Reduced fertility and hypersensitivity to mitomycin C characterize Fancg/Xrcc9 null mice. Hum Mol Genet. 2002;11:273-281.
33. van de Vrugt HJ, Koomen M, Berns MA, et al. Characterization, expression and complex formation of the murine Fanconi anaemia gene product Fancg. Genes Cells. 2002;7:333-342.
34. Blasco MA, Lee HW, Hande MP, et al. Telomere shortening and tumor formation by mouse cells lacking telomerase RNA. Cell. 1997;91:1-3.
35. Herbig U, Jobling WA, Chen PBC, Chen DJ, Sedivy JM. Telomere shortening triggers senescence of human cells through a pathway involving ATM, p53, $p21^{CIP1}$, but not $p16^{INK4a}$. Mol Cell. 2004;501-513.
36. Rufer N, Dragowska W, Thornbury G, et al. Telomere dynamics in lymphocyte subpopulations measured by flow cytometry. Nat Biotechnol. 1998;16:743-747.
37. McIlrath J, Bouffler SD, Samper E, et al. Telomere length abnormalities in mammalian radiosensitive cells. Cancer Res. 2001;61:912-915.
38. Kipling D, Cooke HJ. Hypervariable ultra-long telomeres in mice. Nature. 1990;347:400-402.
39. Hande MP, Samper E, Lansdorp P, Blasco MA. Telomere length dynamics and chromosomal instability in cells derived from telomerase null mice. J Cell Biol. 1999;144:589-601.
40. Yang Y, Kuang Y, De Oca RM, et al. Targeted disruption of the murine Fanconi anemia gene, Fancg/Xrcc9. Blood. 2001;98:3435-3440.
41. Blasco MA, Rizen M, Greider CW, Hanahan D. Differential regulation of telomerase activity and telomerase RNA during multi-stage tumorigenesis. Nat Genet. 1996;12:200-204.
42. Brummelkamp TR, Bernards R, Agami R. A system for stable expression of short interference RNAs in mammalian cells. Science. 2002;296: 550-553.
43. Goytisolo F, Blasco MA. Many ways to telomere dysfunction: in vivo studies using mouse models. Oncogene. 2002;21:584-591.
44. Latre L, Tusell L, Martin M, et al. Shortened telomeres join to DNA breaks interfering with their correct repair. Exp Cell Res. 2003;287:282-288.
45. Collins K, Mitchell JR. Telomerase in the human organism. Oncogene. 2002;21:564-579.
46. Henson JD, Neumann AA, Yeager TR, Reddel RR. Alternative lengthening of telomeres in mammalian cells. Oncogene. 2002;21:598-610.
47. Yamamoto K, Ishiai M, Matsushita N, et al. Fanconi anemia FANCG protein in mitigating radiation- and enzyme-induced DNA double strand breaks by homologous recombination in vertebrate cells. Mol Cell Biol. 2003;23:5421-5430.
48. Aubé M, Lafrance M, Brodeur I, Delisle M-C, Carreau M. Fanconi anemia genes are highly expressed in primitive CD34+ hematopoietic cells. BMC Blood Disord. 2003;3:1-9.
49. Carreau M, Gan OI, Liu L, Doedens M, Dick JE, Buchwald M. Hematopoietic compartment of Fanconi anemia group C null mice contains fewer lineage-negative CD34+ primitive hematopoietic cells and shows reduced reconstruction ability. Exp Hematol. 1999;27:1667-1674.
50. Haneline LS, Gobbett TA, Ramani R, et al. Loss of FancC function results in decreased hematopoietic stem cell repopulating ability. Blood. 1999; 94:1-8.
51. Li X, Plett PA, Yang Y, et al. Fanconi anemia type C deficient hematopoietic stem/progenitor cells exhibit aberrant cell cycle control. Blood. 2003; 102:2081-2084.
52. Hadjur S, Jirik FR. Increased sensitivity of Fancc-deficient hematopoietic cells to nitric oxide and evidence that this species mediates growth inhibition by cytokines. Blood. 2003;101:3877-3884.
53. Allsop RC, Cheshier S, Weissman IL. Telomere shortening accompanies increased cell cycle activity during serial transplantation of hematopoietic stem cells. J Exp Med. 2001;193:917-924.
54. Hemann MT, Strong MA, Hao LY, Greider CW. The shortest telomere, not average telomere length, is critical for cell viability and chromosome stability. Cell. 2001;107:67-77.
55. Samper E, Flores JM, Blasco MA. Restoration of telomerase activity rescues chromosomal instability and premature aging in $Terc^{-/-}$ mice with short telomeres. EMBO Rep. 2001;2:800-807.
56. Wong JC, Alon N, Mckerlie C, Huang JR, Meyn MS, Buchwald M. Targeted disruption of exons 1 to 6 of the Fanconi anemia group A gene leads to growth retardation, strain-specific microphthalmia, meiotic defects and primordial germ cell hypoplasia. Hum Mol Genet. 2003;12:2063-2076.
57. Houghtaling S, Timmers C, Noll M, et al. Epithelial cancer in Fanconi anemia complementation group D2 (Fancd2) knockout mice. Genes Dev. 2003;17:2021-2035.
58. Hemann MT, Rudolph KL, Strong MA, De Pinho RA, Chin L, Greider CW. Telomere dysfunction triggers developmentally regulated germ cell apoptosis. Mol Biol Cell. 2001;12:2023-2030.
59. Allsopp RC, Vaziri H, Patterson C, et al. Telomere length predicts replicative capacity of human fibroblasts. Proc Natl Acad Sci U S A. 1992;89: 10114-10118.
60. Martens UM, Chavez EA, Poon SS, Schmoor C, Lansdorp PM. Accumulation of short telomeres in human fibroblasts prior to replicative senescence. Exp Cell Res. 2000;256:291-299.
61. Ohyashiki JH, Sashida G, Tauchi T, Ohyashiki K. Telomeres and telomerase in hematological neoplasia. Oncogene. 2002;21:680-687.
62. Marciniak R, Guarente L. Testing telomerase. Nature. 2001;413:370-372.
63. Wolthers KC, Bea G, Wisman A, et al. T cell telomere length in HIV-1 infection: no evidence for increased CD4+ T cell turnover. Science. 1996; 274:1543-1547.
64. Notaro R, Cimmino A, Tabarini D, Luzzatto L. In vivo telomere dynamics of human hematopoietc cells. Proc Natl Acad Sci U S A. 1997;94:13782-13785.
65. Pagano G, Youssoufian H. Fanconi anemia proteins: major roles in cell protection against oxidative damage. BioEssays. 2003;25:589-595.
66. Park S-J, Ciccone SLM, Beck BD, et al. Oxidative stress/damage induces multimerization and interaction of Fanconi anemia proteins. J Biol Chem. 2004;279:30053-30059.
67. von Zglinicki T. Oxidative stress shortens telomeres. Trends Biochem Sci. 2002;27:339-344.
68. Garcia-Higuera I, Taniguchi T, Ganesan S, et al. Interaction of the Fanconi anemia proteins and BRCA1 in a common pathway. Mol Cell. 2001;7: 249-262.
69. Hirsch B, Shimamura A, Moreau L, et al. Association of biallelic BRCA2/FANCD1 mutations with spontaneous chromosomal instability and solid tumors of childhood. Blood. 2004;103:2554-2559.
70. Lensch MW, Tishkowitz M, Christianson TA, et al. Acquired FANCA dysfunction and cytogenetic instability in adult acute myelogenous leukemia. Blood. 2003;102:7-16.